The Effect of Ohmic Cable Losses on Time-Domain Reflectometry Measurements of Electrical Conductivity

P. Castiglione* and P. J. Shouse

ABSTRACT

In time domain reflectometry (TDR), the ohmic resistance of the sample medium is related to the amplitude of the reflected signal at long time, once all the multiple reflections have taken place and steady state is achieved. Such a relationship, which permits measuring the sample electrical conductivity, is exact when no signal dissipation occurs other than in the sample. To account for signal attenuation along the coaxial cable, sample and cable are generally modeled as two resistors in series. In this work we review the fundamentals of the transmission line theory and demonstrate, both theoretically and experimentally, that such a formulation is incorrect. We propose a new simple procedure for the analysis of TDR signals based on a difference reflection method, by scaling the reflection coefficients with respect to one or more standards of known conductivity. The procedure was tested on 16 $CaCl_2$ solutions, using two different TDR probes and two cable lengths. The experimental results are in excellent agreement with the theory.

Time domain reflectometry, originally developed by Fellner-Feldegg (1969) in the late sixties and brought to technical maturity especially by the school of Cole (Cole et al., 1980), is employed in a variety of fields for determining the dielectric permittivity of materials over a wide frequency bandwidth. In vadose zone hydrology, it has become an established method for measuring soil water content (θ) and electrical conductivity (σ_a) (Topp et al., 1980; Dalton et al., 1984; Nadler et al., 1991). Due to the ability to perform the two measurements over the same sampling volume, TDR is often preferred over other nondestructive techniques in the investigation of solute transport phenomena as well as for salinity assessment. The attention toward resistivity techniques, and TDR in particular, has increased since the existence of a correlation between electrical and hydraulic conductivity in soils has been recognized (Mualem and Friedman, 1991; Friedman and Seaton, 1998; Purvance and Andricevic, 2000).

Time-domain reflectometry measurements are performed by exciting the sample with a step-like voltage pulse and recording the reflected signal in time domain, the difference between the incident and reflected signal containing information on the dielectric properties of the sample (Nozaki and Bose, 1990). In particular, the electrical conductivity is associated with the signal attenuation, as the voltage pulse sets up current while propagating through a conductive medium and therefore dissipates energy because of the Joule effect (Yeung, 1993). Typical waveforms recorded in deionized water and in $CaCl_2$ solution are shown in Fig. 1, where the signal attenuations are evident for the conductive medium.

Despite a great deal of research, accurate TDR measurement of the soil electrical conductivity has remained a challenge (Huisman and Bouten, 1999), particularly when long coaxial cables are employed, so that additional losses in the signal need to be taken into account. Several researchers (e.g., Dalton et al., 1984; Topp et al., 1988; Yanuka et al., 1988) proposed algorithms for obtaining the direct content (dc) electrical conductivity (σ [dS m^{-1}]) from the analysis of the waveform. Dalton and van Genuchten (1986) related σ to the ratio of the incident (V_i) to the reflected (V_r) voltage at the cable-sample interface, which they located in the waveform as shown in Fig. 1. A similar procedure was proposed by Yanuka et al. (1988), which also takes into account the multiple reflections generated at the sample edges as the signal propagates through the medium.

These early approaches entail the propagation of electromagnetic waves through the soil sample, which represents to a first approximation a section of coaxial transmission line. Besides the uncertainties in locating the voltages in the waveform, such analyses suffer from the simplifying assumptions necessarily introduced to relate σ to the voltage attenuation between different sections of the line. The main reason for this is that other dissipations, mainly those associated with polarization phenomena, affect the voltage attenuation as the signal propagates through the medium. As Buchner et al. (1999) pointed out, only the total dissipation (sum of ohmic and polarization losses) is experimentally accessible with the TDR technique. In theory, therefore, the effects of ohmic losses can only be determined at low frequency, when polarization phenomena vanish. More recently, several authors (e.g., Feng et al., 1999; Heimovaara, 1994) have investigated the frequency dependence of soil dielectric permittivity by determining the S_{11} scatter function of the TDR probe. Although this analysis permits, in principle, measurements of the sample electrical conductivity even in presence of cable losses, it necessarily involves approximate assumptions (for instance, in deriving the mathematical expression for the scatter function, or in the choice of the dispersion model, e.g., Debye's) and parameter optimization. Its use is not justified for electrical conductivity (EC) measurements, which are more simply and more precisely obtained from the zero-frequency analysis of the signal.

The zero-frequency response of the system is readily obtained from the reflected signal at long time, once all

P. Castiglione and P.J. Shouse, George E. Brown Jr. Salinity Laboratory USDA-ARS, 450 W. Big Springs Rd., Riverside, CA 92507. Received 24 May 2002. *Corresponding author (pcastiglione@ussl.ars.usda.gov).

Published in Soil Sci. Soc. Am. J. 67:414–424 (2003).

Abbreviations: dc, direct content; EC, electrical conductivity; TDR, time domain reflectometry.

multiple reflections have taken place and equilibrium is reached. Once fully charged, the sample behaves as an imperfect capacitor, with current leakage proportional to its electrical conductivity. Since the effects of signal propagation vanish at low frequency, the sample can be regarded as a lumped termination of the transmission line, whose electrical resistance R_s (Ω) is measured accurately from the long-time reflected voltage (Nadler et al., 1991). The sample conductivity (σ) is then obtained from:

$$R_s = \frac{K_p}{\sigma} \qquad [1]$$

where the probe constant K_p (m^{-1}) can be determined from calibration with standards of known conductivity.

The lumped element, or zero-frequency analysis is exact for ideal systems, for which ohmic losses only occur within the investigated sample. To account for additional attenuations due to the cable, connectors and multiplexer, which are never negligible in practical applications, Heimovaara et al. (1995) suggested that cable and sample can be modeled as resistors in series whose electrical resistances are R_{cable} and R_s, respectively. The system is in this case fully characterized by two parameters, K_p and R_{cable}, which can be obtained from least squares fitting of calibration data in electrolytic solutions. Recently, Reece (1998) observed discrepancies between optimized and independently measured values of K_p and R_{cable}. In his analysis, the probe constant was calculated by assuming the sample to be a section of coaxial line, whereas R_{cable} was measured precisely by applying the lumped analysis to different segments of coaxial cables. Similar inconsistencies were reported by Huisman and Bouten (1999) by comparing measured vs. optimized R_{cable} values. They suggested that, "the theory is incomplete and the fitting procedures correct for the deviations from theory."

We believe that a rigorous analysis of TDR measurements of electrical conductivity is still largely missing, and that the general validity of the technique is often not fully recognized. In this paper, we review the principal theoretical aspects of the technique and show, both theoretically and experimentally, that the series resistances assumption is incorrect. To accurately account for the cable losses, we propose a simple procedure for the analysis of the signal, based on the difference reflection method. The procedure was tested on 16 $CaCl_2$ solutions at different concentrations, using two different TDR probes and two cable lengths.

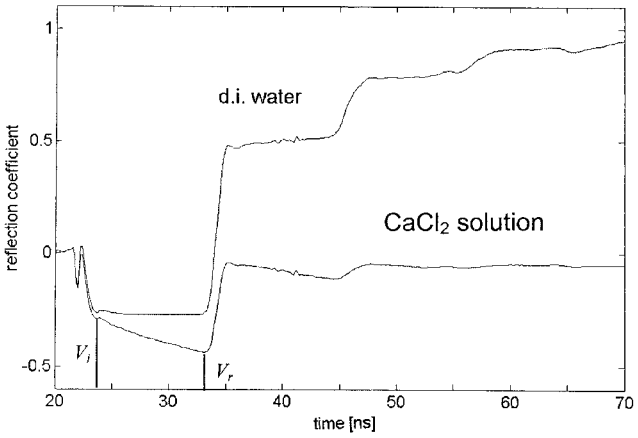

Fig. 1. Time domain reflectometry waveforms recorded with a 20-cm probe. The reflection coefficient is defined as the ratio of the incident to the reflected voltage. Because of the ohmic dissipation, the signal undergoes attenuations when propagating through the conductive (σ = 0.68 dS m^{-1}) $CaCl_2$ solution.

THEORY

In TDR, the sample dielectric is usually placed in a section of transmission line of length d at the end of a coaxial cable, as shown in Fig. 2. A fast rising step voltage produced by a tunnel diode is transmitted through the cable to the sample and reflected back to the generator, where it is completely absorbed. The incident (V_i) and reflected (V_r) voltages are then recorded in the time domain by a fast sampling oscilloscope, and processed. In a typical configuration, the probe represents an open-ended coaxial line, whose input impedance is given by (Cole and Winsor, 1982):

$$Z_{in}(\omega) = Z_g \frac{c}{d} \frac{1}{j\omega} \frac{z\cot z}{\varepsilon_t} \qquad [2]$$

where ε_t is the total relative permittivity of the dielectric filling the cell:

$$\varepsilon_t(\omega) = \varepsilon'(\omega) - j\varepsilon''(\omega) + \frac{\sigma}{j\omega\varepsilon_0} \qquad [3]$$

In the equations above, $j^2 = -1$; ω is the angular frequency $2\pi f$; c is the speed of light (3×10^8 m s^{-1}); Z_g the characteristic impedance of the empty sample ($\varepsilon_t = 1$), here referred to as geometric impedance; $\varepsilon'(\omega)$ is the real part of the relative dielectric permittivity; in the imaginary part of Eq. [3], $\varepsilon''(\omega)$ accounts for the relaxation losses, while σ, the dc electrical conductivity of the sample, for the ohmic losses; ε_o is the dielectric permittivity of free space (8.8542×10^{-12} F m^{-1}) and $z = (\omega d/c)\sqrt{\varepsilon_t}$.

At any section of a transmission line, the input impedance is defined as the ratio of the voltage (v) to the current (i) Laplace transforms. From transmission line theory, therefore, the impedance in Eq. [2] can also be expressed as (Wolff and Kaul, 1988):

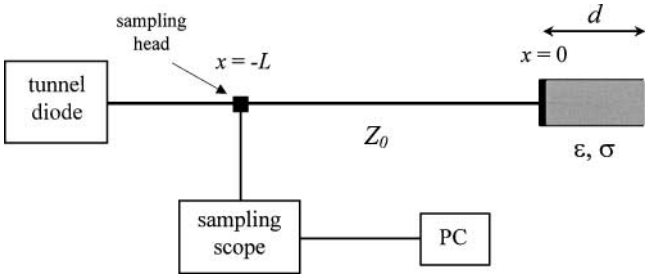

Fig. 2. Schematic representation of the time domain reflectometry setup. The sample dielectric of length d is placed at the end of a coaxial cable of length L and characteristic impedance Z_0, and is excited with a step voltage produced by the tunnel diode. From the reflected signal, recorded in the time domain by a sampling scope and processed with a personal computer, it is possible to obtain the dielectric properties of the sample (ε, σ).

$$Z_{in}(\omega) = \frac{v(\omega)}{i(\omega)} = Z_0 \frac{v_i(\omega) + v_r(\omega)}{v_i(\omega) - v_r(\omega)} \quad [4]$$

where v_i and v_r are respectively the Laplace transforms of the incident and reflected voltages at the separation plane between the coaxial cable and the cell ($x = 0$, in Fig. 2):

$$v_i(\omega) = L[V_i(t)] = \int_0^\infty \exp(j\omega t)\, V_i(t)dt \quad [5]$$

and Z_0 is the characteristic impedance of the cable, generally equal to 50 Ω. Resolving Eq. [2] and [4] we obtain:

$$\varepsilon_t = \frac{Z_g}{Z_0} \frac{c}{d} \frac{1}{j\omega} \frac{v_i - v_r}{v_i + v_r} z\cot z \quad [6]$$

Equation [6] represents a basic equation in spectroscopy (Cole et al., 1980), as it relates the frequency-dependent permittivity of the dielectric to the transforms of the incident and reflected signal. It is important to point out that the voltages, v_i and v_r, in Eq. [7] are at the cable-sample interface ($x = 0$), and generally differ from the actual measured voltages at the sampling head (i.e., at $x = -L$ in Fig. 2).

The "propagation factor" $z\cot z$ accounts for multiple reflections generated at the probe edges as the signal propagates through the medium. These correspond to the z-dependent terms in the series expansion (Cole and Winsor 1982):

$$z\cot z = 1 - \frac{1}{3} z^2 - \frac{1}{45} z^4 + \ldots \quad [7]$$

valid for $|z| < 1/2\pi$. For very thin samples ($d \to 0$) the effects of the multiple reflections can be neglected, as $z \to 0$ and the term $z\cot z \to 0$. In this case, the propagation of the signal through the probe is instantaneous, that is, the sample behaves as a lumped element. Notice from the expression for z that the same result is valid at low frequency, as $z \to 0$ for $\omega \to 0$. At low frequency, therefore, the probe can be regarded as a lumped element. This is physically sound since at low frequency the sample length is a small fraction of the wavelength ($<\lambda/10$), and voltage and current variations along the probe become negligible. We therefore can rewrite Eq. [6] for low frequency as follows:

$$\varepsilon' - j\varepsilon'' + \frac{\sigma}{j\omega\varepsilon_0} = \frac{Z_g}{Z_0} \frac{c}{d} \frac{1}{j\omega} \frac{v_i - v_r}{v_i + v_r} \quad [8]$$

Multiplying both terms of Eq. [8] by $j\omega$, and recalling that $j\omega v = L(dV/dt)$, we have:

$$j\omega(\varepsilon' - j\varepsilon'') + \frac{\sigma}{\varepsilon_0} = \frac{Z_g}{Z_0} \frac{c}{d} \frac{\int_0^\infty \exp(j\omega t) \frac{d}{dt}[V_i(t) - V_r(t)]dt}{\int_0^\infty \exp(j\omega t) \frac{d}{dt}[V_i(t) + V_r(t)]dt} \quad [9]$$

which, in the limit $\omega \to 0$, becomes:

$$\frac{\sigma}{\varepsilon_0} = \frac{Z_g}{Z_0} \frac{c}{d} \frac{V_i(\infty) - V_r(\infty)}{V_i(\infty) + V_r(\infty)} \quad [10]$$

If we let ρ_∞ be the reflection coefficient at infinite time:

$$\rho_\infty = \frac{V_r(\infty)}{V_i(\infty)} \quad [11]$$

we can rewrite Eq. [10] in the more familiar form:

$$\sigma = \frac{1}{Z_0} \frac{\varepsilon_0 c Z_g}{d} \frac{1 - \rho_\infty}{1 + \rho_\infty} \quad [12]$$

Based on the work of Giese and Tiemann (1975), Eq. [12] was first proposed by Topp et al. (1988).

Since the lumped element analysis is rigorous at low frequency, as we observed, we can readily calculate the sample resistance (R_s) for generically shaped probes. R_s (Ω) represents in fact the zero frequency impedance of a lumped termination of the coaxial cable. Equating the input impedance in Eq. [4] to R_s, and taking the limit $\omega \to 0$ as done before, we obtain:

$$R_s = \frac{K_p}{\sigma} = Z_0 \frac{V_i(\infty) + V_r(\infty)}{V_i(\infty) - V_r(\infty)} \quad [13]$$

where K_p (m^{-1}) is the probe constant. Equation [13], first proposed by Nadler et al. (1991), is valid for a generic termination of the coaxial cable; if this is a section of coaxial line, Eq. [10] and [13] are equivalent, as pointed out by Heimovaara (1992). Equating these two leads to the following expression for the probe constant:

$$K_p = \frac{\varepsilon_0 c Z_g}{d} \quad [14]$$

Difference Reflection Method

Since the incident voltage pulse is very difficult to measure accurately (Cole et al., 1980), a common technique in time domain spectroscopy is to compare the signals reflected from the sample filled with the unknown dielectric and with a reference medium of known dielectric properties. At low frequency, this analysis permits comparing the electrical conductivities of the two media. Rewriting Eq. [10] for the investigated (subscript x) and the reference dielectric (subscript r) and subtracting, we obtain:

$$\frac{\sigma_x}{\varepsilon_0} - \frac{\sigma_r}{\varepsilon_0} = \frac{Z_g}{Z_0} \frac{c}{d} \frac{V_{r,r}(\infty) - V_{r,x}(\infty)}{V_{r,r}(\infty) + V_{r,x}(\infty)} \quad [15]$$

where $V_{r,r}(\infty)$ and $V_{r,x}(\infty)$ are reflected voltages at infinite time, relative to the reference and the unknown dielectric respectively. Taking air as the reference dielectric ($\sigma_r = 0$), we obtain from Eq. [15]:

$$R_s = \frac{K_p}{\sigma_x} = Z_0 \frac{V_{r,r} + V_{r,x}}{V_{r,r} - V_{r,x}} = Z_0 \frac{1 + \rho_2}{1 - \rho_2} \quad [16]$$

with $\rho_2 = V_{r,x}/V_{r,r}$ and the probe constant given by Eq. [14].

Effect of Cable Losses

In the analysis thus far, the dielectric properties of the sample were related through a simple mathematical expression (Eq. [6]) to the voltage at the cable-sample interface ($x = 0$). However, the voltage is actually measured at the sampling head ($x = -L$), so that the propagation of the signal along the coaxial cable needs to be taken into account. For ideal (lossless) cables the problem is trivial since the input impedance in Eq. [4] is uniform (Wolff and Kaul, 1988) and all of the equations above remain valid when the measured voltage replaces the voltage at the interface. For the general case, the input impedances at the measuring plane and at the interface are related by a bilinear transformation, whose complex coefficients are determined from measurements with standards of known permittivity (see for example Bertolini et al., 1991).

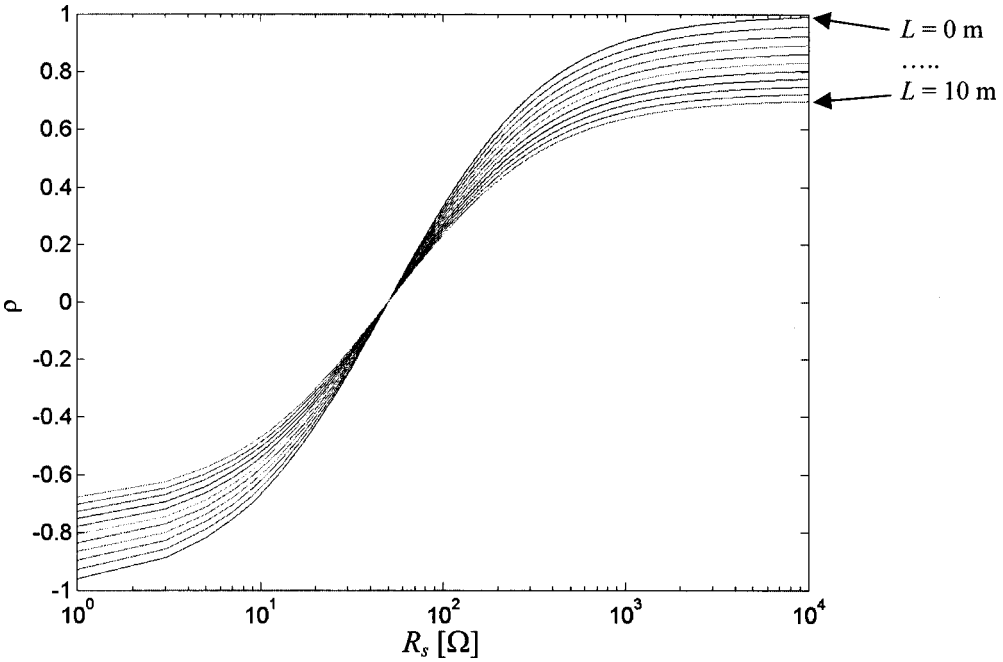

Fig. 3. Dependence of the measured reflection coefficients (ρ) on the sample resistance (R_s) and length (L) of an RG 58A/U coaxial cable (α = 0.0175). A = 1 for L = 0 m, while for L = 10 m A = 1.419. Note that no reflection occurs for R_s = 50 Ω.

Since we are only interested in the zero-frequency response of the system, the analysis can be greatly simplified. To keep notations simple, measured voltages are identified in the following with an over bar (i.e., $V(-L,\infty) = \overline{V}$), while the usual notation is reserved for voltages at the cable-sample interface (i.e., $V(0,\infty) = V$). Because of ohmic dissipations, the steady-state (i.e., at the infinite time) voltage varies exponentially along a uniform transmission line (Grant and Phillips, 1990). Hence, if x_1 and x_2 are two generic sections of the line, we have:

$$V(x_2, \infty) = V(x_1, \infty)\exp[-\alpha(x_2 - x_1)] \qquad [17]$$

where α is the attenuation coefficient of the line. By disregarding the effects of connectors, multiplexer, and other discontinuities between the sampling head and the probe, we can therefore write:

$$\overline{V}_i = V_i\exp(\alpha L) \quad \overline{V}_r = V_r\exp(-\alpha L) \qquad [18]$$

Notice that the sign of the exponent changes with the direction of propagation of the signal. By substituting Eq. [18] in Eq. [13], we obtain:

$$\begin{aligned} R_s &= Z_0\frac{\overline{V}_i\exp(-\alpha L) + \overline{V}_r\exp(\alpha L)}{\overline{V}_i\exp(-\alpha L) - \overline{V}_r\exp(\alpha L)} \\ &= Z_0\frac{\overline{V}_i + \overline{V}_r\exp(2\alpha L)}{\overline{V}_i - \overline{V}_r\exp(2\alpha L)} \\ &= Z_0\frac{\overline{V}_i + \overline{V}_r A}{\overline{V}_i - \overline{V}_r A} = Z_0\frac{1 + \overline{\rho}A}{1 - \overline{\rho}A} \end{aligned} \qquad [19]$$

which relates R_s to the measured reflection coefficient ($\overline{\rho}$) and to the attenuation constant A = exp(2αL). The constant A accounts for signal losses over a path of length $2L$, and equals 1 for ideal cables (α = 0). Equation [19] can also be derived from the difference reflection method. Substituting the last of Eq. [18] into Eq. [16] we have in fact:

$$R_s = Z_0\frac{V_{r,r} + V_{r,x}}{V_{r,r} - V_{r,x}} = Z_0\frac{\overline{V}_{r,r}\exp(-\alpha L) + \overline{V}_{r,x}\exp(-\alpha L)}{\overline{V}_{r,r}\exp(-\alpha L) - \overline{V}_{r,x}\exp(-\alpha L)}$$

$$= Z_0\frac{\overline{V}_{r,r} + \overline{V}_{r,x}}{\overline{V}_{r,r} - \overline{V}_{r,x}} = Z_0\frac{1 + \overline{\rho}_2}{1 - \overline{\rho}_2} \qquad [20]$$

Notice that $\overline{\rho}\,A = \overline{\rho}_2$ (with air as a reference medium), and therefore the Eq. [18] and [19] are equivalent. In other words, in the hypothesis of Eq. [18], to account for the cable losses one either needs to estimate the attenuation constant A to be used in Eq. [19], or to compare the signals reflected from the unknown dielectric and from the probe in air (which undergo the same attenuation along the cable) by using Eq. [20].

The introduction of the attenuation constant allows us to clearly discriminate the attenuations due to the sample and the cable. The measured reflection coefficient at long time depends in fact on the sample resistance (R_s) and on the characteristics of the cable (embedded in the constant A) according to:

$$\overline{\rho} = \frac{1}{A}\frac{R_s - Z_0}{R_s + Z_0} \qquad [21]$$

which is obtained by rearranging Eq. [19]. Given the attenuation coefficient of the cable (α), A depends only on the cable length (A = exp [2αL]). For example, the commonly used RG 58A/U coaxial cable displays an attenuation of about 0.15 dB m^{-1} at 100 Mhz[1] (Sinnema, 1979), which corresponds to an attenuation coefficient α of 0.152 dB (0.0175 Neper). With this value we calculated the attenuation constants A for different cable lengths ($0 \le L \le 10$ m) and plotted the results of Eq. [21] in Fig. 3. Clearly, the curve correspondent to L = 0 represents the case of lossless cable. It appears that, for any sample resistance, the absolute value of the reflection coefficient decreases with the cable length. The cable effects are greater for highly conductive samples (small R_s) and for very high sample resistances. For R_s = 50 Ω no reflection occurs ($\overline{\rho}$ = 0) independently on the cable length, as the line is matched.

[1]The reported value can be regarded as the dc attenuation.

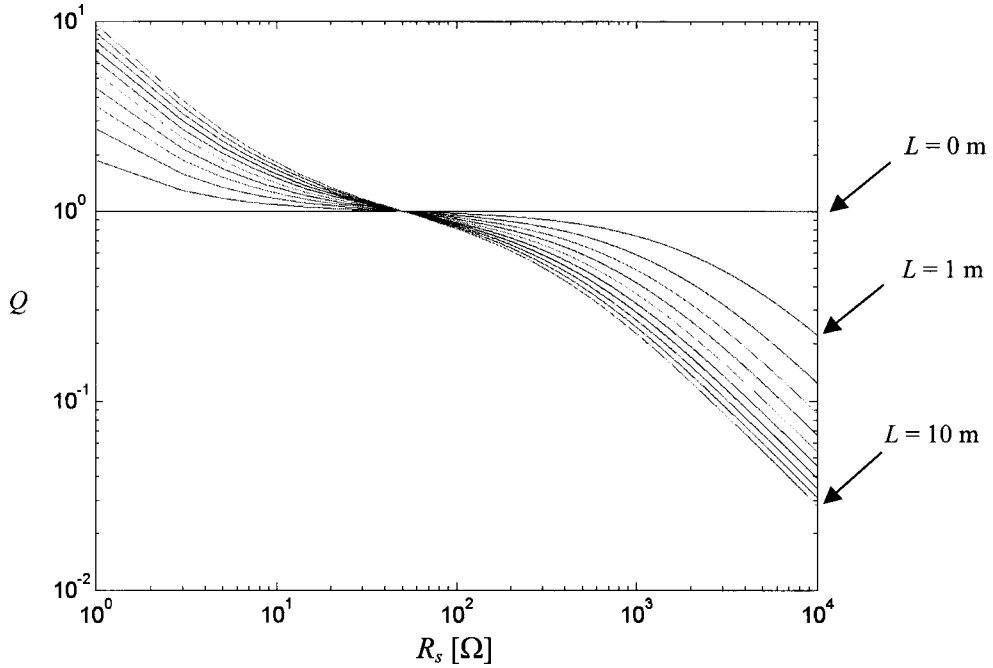

Fig. 4. Expected relative errors in R_s measurements when neglecting the cable losses. $Q = R_{s,a}/R_s$, with $R_{s,a}$ given in Eq. [22]. The relative error becomes negligible as $|R_s|$ approaches $Z_0 = 50$ Ω.

We can now predict the errors expected in the measurement of sample resistance when the cable losses are neglected. By substituting the reflection coefficient given in Eq. [21] in Eq. [13], we obtain an apparent sample resistance:

$$R_{s,a} = Z_0\left(1 + \frac{1}{A}\frac{R_s - Z_0}{R_s + Z_0}\right)\Big/\left(1 - \frac{1}{A}\frac{R_s - Z_0}{R_s + Z_0}\right) \quad [22]$$

which is calculated by ignoring the cable attenuations. In Fig. 4, we plotted the ratio between the apparent and the effective sample resistance ($Q = R_{s,a}/R_s$) against R_s for different values of cable length. It is interesting to note that ignoring cable losses leads to overestimating the sample resistance for $R_s <$ 50 Ω, and to underestimating the sample resistance for $R_s >$ 50 Ω. In any case, it is apparent that, even for very short cables, the errors can be unacceptable in the extremes of very conductive and very resistive samples.

A last observation concerns with the reflection coefficients measured in air ($R_s = \infty$) and in short circuited probe ($R_s =$ 0). Form Eq. [19] follows:

$$\bar{\rho}_{air} = 1/A \qquad \bar{\rho}_{sc} = -1/A \quad [23]$$

For lossy cables (A > 1), therefore, these reflection coeficients are <1 in absolute value.In contrast, from Eq. [20]:

$$\bar{\rho}_{air} = 1/A \qquad \bar{\rho}_{sc} = -1/A \quad [24]$$

Therefore, once scaled with respect to the waveform in air, the reflection coefficients measured in air and in short-circuited probe equal 1 in absolute values, even in presence of cable losses. Equation [23] permits estimating the attenuation constant from measurements of either $\bar{\rho}_{air}$ or $\bar{\rho}_{sc}$. As we will show when discussing the experimental results, the Eq. [18] may not hold in presence of connectors, multiplexer, or other discontinuities between the measuring plane and the cable-sample interface. Equation [23] may therefore be not accurate, and $\bar{\rho}_{air}$ and $\bar{\rho}_{sc}$ may even differ in absolute value. In this case it is convenient to use a second-reference medium, besides air, in the analysis of the waveforms. For instance, we can scale $\bar{\rho}$ with respect to the values measured in air ($\bar{\rho}_{air}$) and in the short-circuited probe ($\bar{\rho}_{sc}$) as follows:

$$\bar{\rho}_3 = 2\frac{\bar{\rho} - \bar{\rho}_{air}}{\bar{\rho}_{air} - \bar{\rho}_{sc}} + 1 \quad [25]$$

The new reflection coefficient $\bar{\rho}_3$ equals 1 for nonconductive samples ($\bar{\rho} = \bar{\rho}_{air}$) and −1 for short-circuited probes ($\bar{\rho} = \bar{\rho}_{sc}$), (as is the case for lossless cables), independently on the validity of Eq. [18]. This procedure was first adopted by Dalton (1992), even though he did not fully appreciate the general validity of the lumped element analysis.

Series Resistors Model

This simple analysis also allows us to investigate the assumption, generally adopted in soil science, that the coaxial cable and the sample can be modeled as two resistors in series (Heimovaara et al., 1995). More precisely, it is assumed that:

$$Z_0\frac{\bar{V}_i + \bar{V}_r}{\bar{V}_i - \bar{V}_r} = R_{tot} = R_s + R_{cable} \quad [26]$$

where R_{cable} represents the sum of the resistance due to cable, multiplexer, and connectors. Indicating $R_{tot} = 1/G_1$, and as usual $R_s = K_p/\sigma$, Eq. [26] is rewritten as:

$$\frac{\sigma}{G_1} = K_p + \sigma R_{cable} \quad [27]$$

Based on Eq. [27], Heimovaara et al. (1995) suggested that the data measured on electrolytic solutions of known conductivity should lie on a straight line when plotted as σ/G_1 against

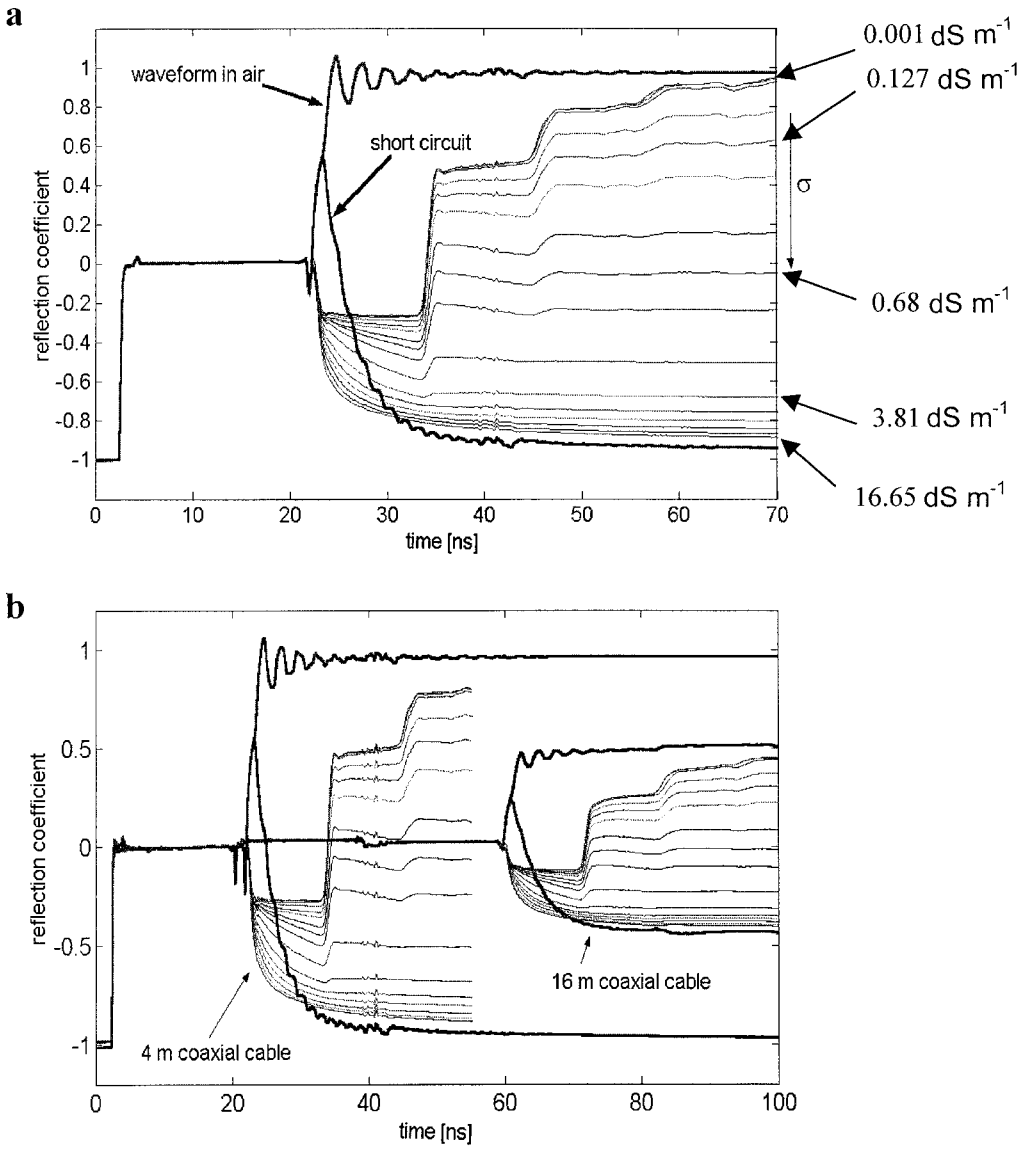

Fig. 5. Waveforms recorded in electrolytic solutions with the 20-cm probe connected to (a) the 4-m long coaxial cable and to both (b) the 4- and the 16-m cables. In both cases the reflection coefficients reach a flat plateau after few reflections. The long-time reflection coefficients to be used in the Eq. [32] through [34] is measured at about 600 ns.

σ, and that the parameters K_p and R_{cable} could be obtained from the intercept and slope of the interpolating line, respectively.

We will demonstrate that the hypothesis expressed by Eq. [26] is unrealistic, and that the procedure suggested by Heimovaara et al. (1995) leads to incorrect estimates of the cable resistance. By using the expression for R_s in Eq. [12], we can rewrite Eq. [26] as follows:

$$R_{cable} = Z_0 \frac{\overline{V}_i + \overline{V}_r}{\overline{V}_i - \overline{V}_r} - Z_0 \frac{V_i + V_r}{V_i - V_r} \qquad [28]$$

Assuming valid Eq. [18], we obtain by substitution:

$$R_{cable} = Z_0 \frac{2V_iV_r\,(1 - A)}{(V_i - V_r)(AV_i - V_r)} \qquad [29]$$

and since from Eq. [13] $V_r = V_i(R_s - Z_0)/(R_s + Z_0)$, we have:

$$R_{cable} = \frac{(R_s^2 - Z_0^2)(1 - A)}{R_s\,(A - 1) + Z_0\,(A + 1)} \qquad [30]$$

This expression suggests that the cable resistance is determined not only by quantities characteristic of the cable (such as Z_0 and A), but also by the sample resistance R_s, which is clearly non–physical. This is because the hypothesis of series resistances, although intuitive, does not hold for the cable-sample system. When discussing the experimental results, we will quantify the expected errors when Eq. [30] is used for a real case.

MATERIALS AND METHODS

Time domain reflectometry measurements were made on 16 $CaCl_2$ electrolytic solutions, with σ varying from 0.001 to 16.65

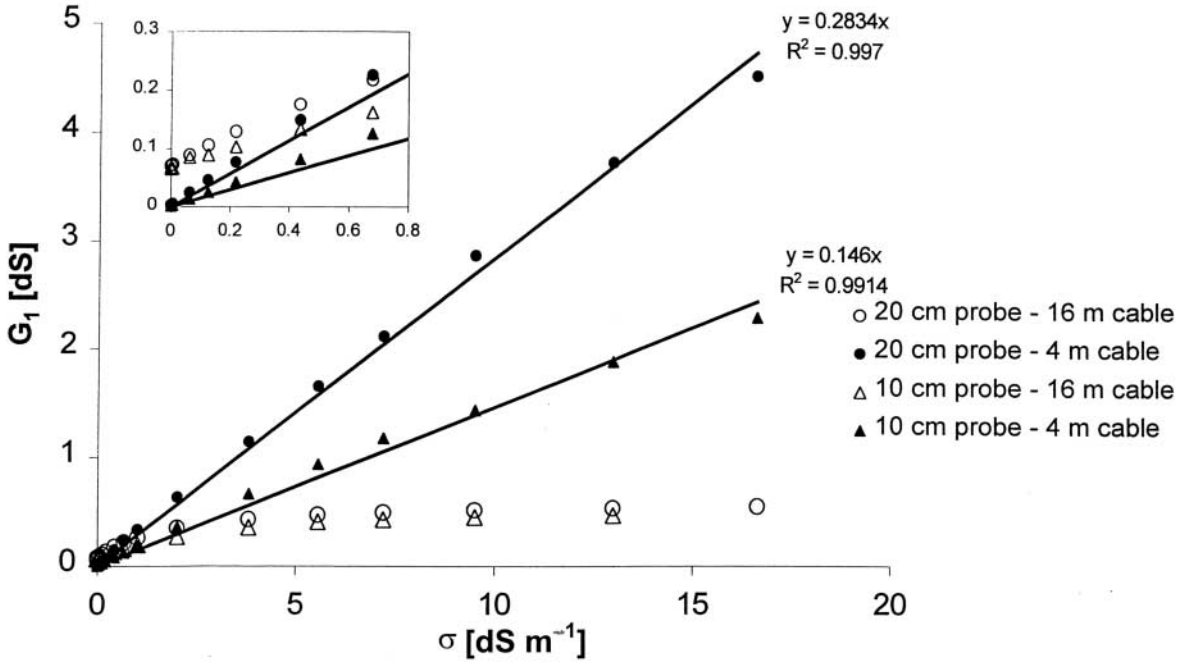

Fig. 6. Sample conductance calculated with the lossless cable model (Eq. [32]). The hypothesis is reasonable when using the 4-m long cable, whereas it is unrealistic for the 16-m cable, as the relative data fail to align on a straight line.

dS m^{-1}. The electrical conductivity was measured independently with a standard EC meter (YSI-32 Yellow Spring Int. Inc., Yellow Sping, OH). For each solution, measurements were taken with two different probes (10 and 20 cm long) and two 50-Ω coaxial cables (RG 58A/U), 4 and 16 m long respectively. In the 16-m cable configuration, a multiplexer (SDMX 50Ω Campbell Sci. Inc., Logan, UT) was interposed between 4- and 12-m long cables. Both TDR probes emulate coaxial geometry with a three-rod configuration (Zegelin et al., 1989); the inter-rod spacing was 0.8 cm for the 10-cm probe and 1.5 cm for the 20-cm probe. For each probe-cable configuration, we also recorded waveforms in air and with the probe short-circuited (aluminum foil was placed at the end of the metallic rods).

For our measurements we used a Tektronix 1502B cable tester, controlled through an RS232 serial port interface (SP232 Tektronix, Tektronix, Beaverton, OR) by a personal computer. A special code (Heimovaara, 1994) allowed us to collect 16 384 point waveforms, so that both the high and the low frequency range could be traced in a single measurement (with the distance/division ratio set equal to 0.5, and the velocity of propagation set to 0.66, as default). The waveforms were analyzed with Matlab to determine the reflection coefficient at long time ($\bar{\rho}_\infty$) from an average of 200 points at about 600 ns (a flat plateau was already reached after about 60 ns; see Fig. 3a as an example).

RESULTS AND DISCUSSION

Typical waveforms recorded in electrolytic solutions are shown in Fig. 5a, where the reflection coefficients ($\bar{\rho}$) measured with the 20-cm probe and the 4-m coaxial cable are plotted against time. In the same figure we also show the waveforms corresponding to the probe in air and the short-circuited probe. At long time, the reflection coefficient approaches the value measured in air for the lowest solute conductivity, while it drops close to the value corresponding to the short-circuited probe as the conductivity increases. Cable-loss effects are evident when comparing the waveforms recorded with the 4- and 16-m coaxial cables (Fig. 5b). In both cases, the long-time reflection coefficients measured in the electrolytic solutions lie between two extreme values, corresponding to the probe in air and the short-circuited probe. As predicted by Eq. [21], these values are reduced in absolute value because of the cable attenuation. In particular, the reflection coefficient in air is very close to 1 for the 4-m cable, while it is reduced to about 0.5 for the 16-m cable.

According to the models described earlier, we calculated the sample resistance from the reflection coefficients measured at long time. A simple way to test the different approaches is by plotting the sample conductance:

$$G_s = 1/R_s = \sigma/K_p \text{ [dS]} \qquad [31]$$

against the independently measured conductivity of the electrolytic solutions (σ [dS m^{-1}]). Based on Eq. [31], properly measured G_s values should lie on a straight line intercepting the origin, whose slope equals the reciprocal of the probe constant, and is therefore independent of the cable length. Any deviation from such behavior reflects limitations in the model.

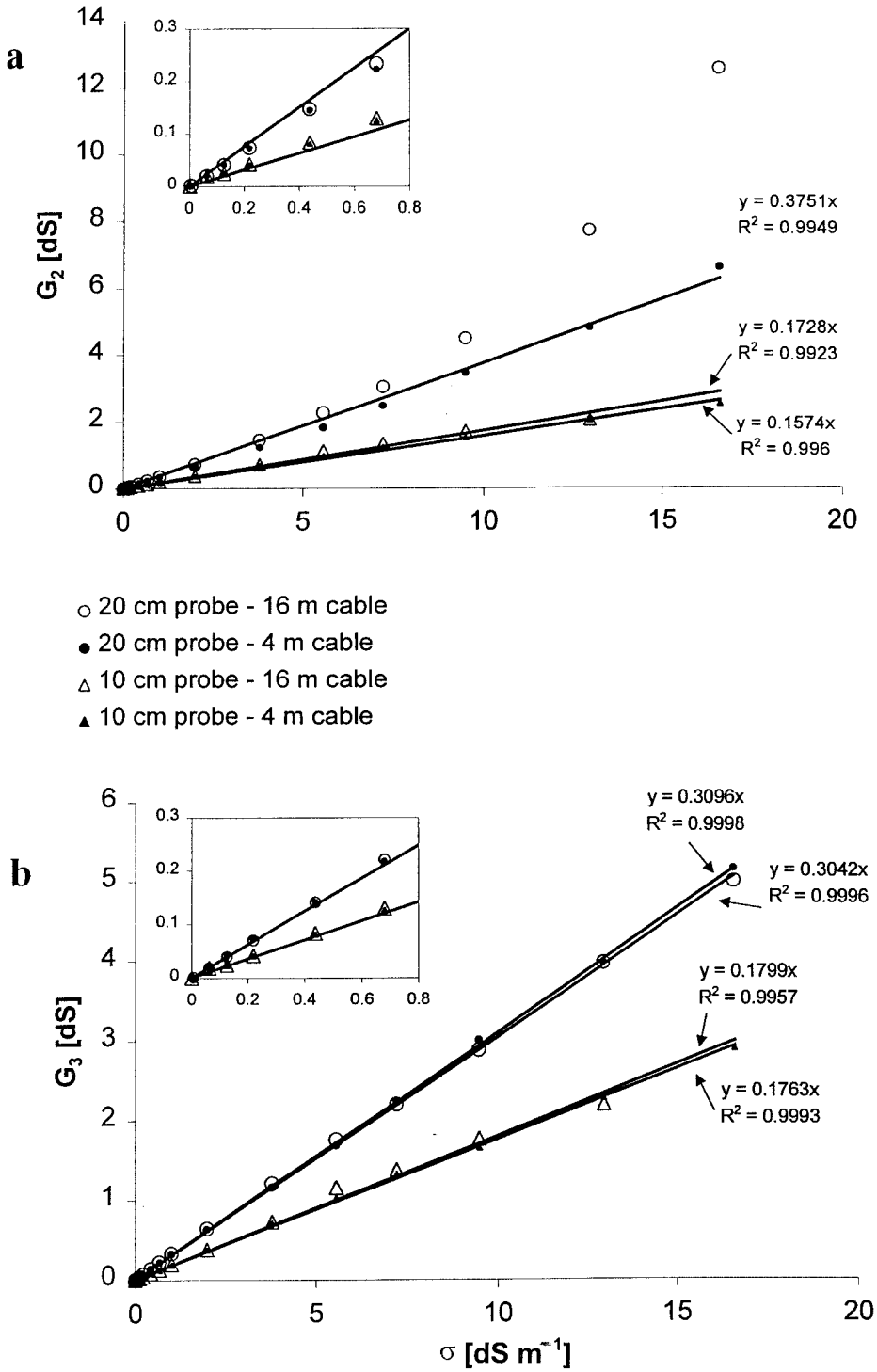

Fig. 7. Sample conductance calculated by scaling the reflection coefficients with respect to the waveform measured in (a) air, and to both (b) the waveform in air and with the probe short-circuited.

At first we neglected any cable effect by calculating the sample conductance:

$$G_1 = \frac{1}{Z_0}\frac{1-\bar{\rho}}{1+\bar{\rho}} \qquad [32]$$

from Eq. [19], with $A = 1$. This expression can also be obtained from Eq. [12] recalling that $\rho = \bar{\rho}$ for ideal cables. G_1 is plotted in Fig. 6 against σ. While the data corresponding to the 4-m cable are roughly aligned on a straight line, G_1 appears to be nonlinearly related to σ when using the 16-m cable, thus demonstrating the inadequacy of the lossless cable assumption. We then tested

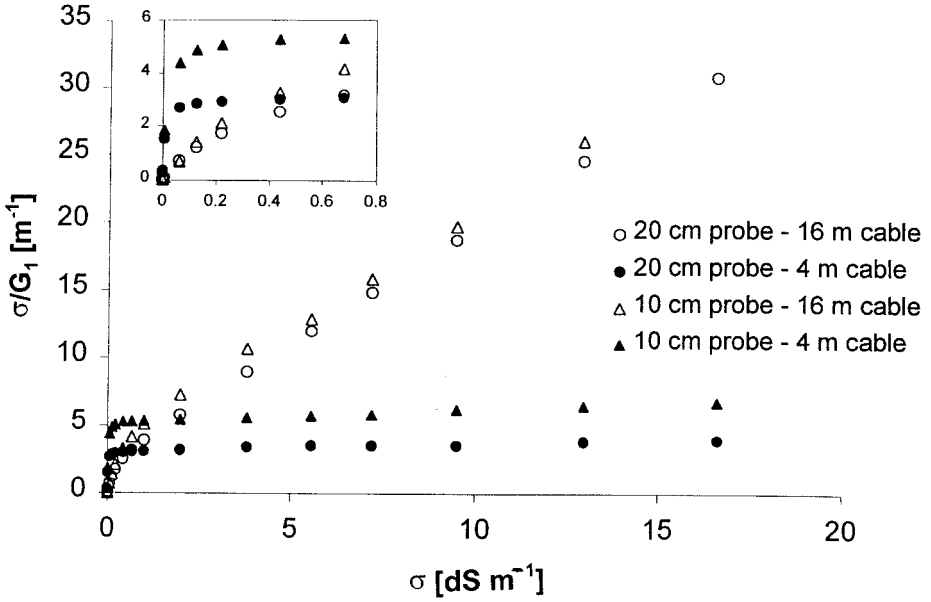

Fig. 8. G_1 **is the sample conductance assuming cable and sample as resistors in series; the solution conductivity σ is independently measured with a standard meter. The limitations of the model are only evident in the low conductivity range.**

the difference reflection method (Eq. [20]), with air as the reference dielectric, by plotting G_2 against σ, where

$$G_2 = \frac{1}{Z_0}\frac{1-\bar{\rho}_2}{1+\bar{\rho}_2} \quad [33]$$

Figure 7a shows that this method works reasonably well for the 10-cm probe, in that the data for the 4- and 16-m cables lie on the same line, whereas it fails for the 20-cm probe; in this case the data corresponding to the 16-m cable diverge from a straight line as the sample conductivity increases. This result may be ascribed to the approximate nature of Eq. [18], which does not take into account the presence of the multiplexer in the long cable configuration. The limitations in the model are also evident from the analysis of the waveforms, since $\bar{\rho}_{air}$ and $\bar{\rho}_{sc}$ slightly differ in absolute value, contrary to what Eq. [23] predicts.

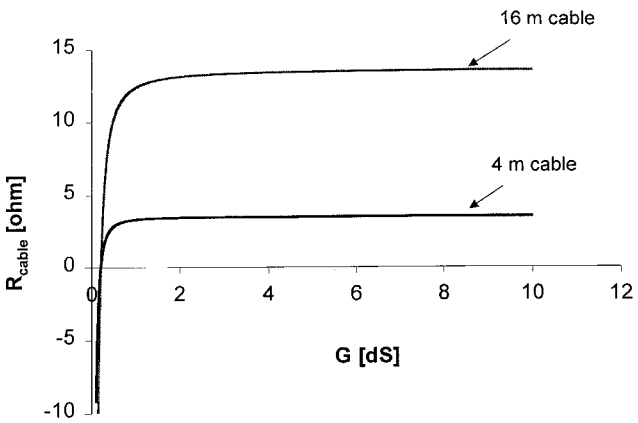

Fig. 9. R_{cable} **predicted by the series resistance model (Eq. [23]) for the RG 58A/U cable. When the sample conductance** G **is not too small (>1 dS),** R_{cable} **appears to be constant and the data from the calibration appears to be aligned on a straight line.**

To account more precisely for the additional losses, we scaled $\bar{\rho}$ with respect to the values measured in air ($\bar{\rho}_{air}$) and in the short-circuited probe ($\bar{\rho}_{sc}$), according to the transformation [25]. The sample conductance defined as:

$$G_3 - \frac{1}{Z_0}\frac{1-\bar{\rho}_3}{1+\bar{\rho}_3} \quad [34]$$

is plotted against σ in Fig. 7b. All data in this case lie on a straight line, whose slope is only dependent on the sample geometry. We calculated $K_p = 5.62\ m^{-1}$ for the 10-cm probe, and $K_p = 3.26\ m^{-1}$ for the 20-cm probe. We therefore recommend using Eq. [34], with the transformation [25], for accurate measurements of the sample resistance. Once the cable losses are properly accounted for, the probe constant can be obtained from measurement in only one electrolytic solution of known conductivity. We found that such a probe calibration is rapid and accurate, whereas use of theoretical Eq. [14] to calculate the probe constant is not justified, because of simplifying assumption in the coaxial cell model, and uncertainties in the determination of the geometric impedance (Spaans and Baker, 1993).

The collected data also allowed us to test the series resistance hypothesis (Eq. [21]) by plotting σ/G_1 against σ (Fig. 8). It is apparent that each series of data fails to lie on a straight line in the low conductivity range. R_{cable}, which for Eq. [27] is the slope of the interpolating curve, thus appears to be dependent on the sample resistance, as we had mentioned earlier when introducing Eq. [30]. The nature of this dependence can be highlighted by specifying a value for the constant A in Eq.

[30]. For $\alpha = 0.152$ Db (0.0175 Np) (characteristic of the RG 58A/U coaxial cable, as we found earlier), we calculated the attenuation constants for the 4-m ($A = 1.053$) and 16-m ($A = 1.874$) cables. The corresponding R_{cable} values calculated from Eq. [30] are plotted in Fig. 9 against the sample conductance G [dS]. R_{cable} appears to be constant for a wide range of G values, while it drops for small values of the sample conductance until it reaches meaningless negative values for $G < 0.2$ (corresponding to $R_s = 50\ \Omega$).

We noticed that truncating the series of data for $G <$ 1 dS (i.e., disregarding the nonlinear portions of the curves in Fig. 8), the values of R_{cable} estimated from the slope of the interpolating line are in close agreement with the values corresponding to the flat portions of the curves in Fig. 9. Averaging the values obtained for the two probes, we found $R_{cable} = 16.7\ \Omega$ for the 16-m cable, and $R_{cable} = 1.2\ \Omega$ for the 4-m cable. This observation suggests that if the sample conductance employed in the calibration procedure is not too small (e.g., <1 dS), the data plotted for Eq. [27] actually lie on a straight line, so that the limitations of the model are not apparent. This explains why the model suggested by Heimovaara et al. (1995), although conceptually incorrect, works reasonably well in terms of accounting for cable losses, as long as the conductivity of the investigated sample is not too small.

CONCLUSION

We demonstrated that the lumped element analysis is rigorous at low frequency, and that the sample resistance is related to the long-time voltage at the cable-sample interface by an exact relationship. If, at zero frequency, the voltage is distributed exponentially along the cable, the effects of the cable losses are readily accounted for by scaling the reflection coefficients with the waveform recorded in air. However, because of connectors, the multiplexer, and other discontinuities between the TDR probe and the sampling scope, this condition is not generally met. We found that cable losses are best accounted for when the reflection coefficients are scaled with respect to both the waveform in air and with the probe short-circuited. In this way, the probe constant is readily obtained by calibrating the instrument in standard electrolytic solutions of known conductivity. We also showed, both theoretically and experimentally, that cable and sample cannot be modeled as resistors in series, as commonly done, and that the relative calibration procedure leads to incorrect measurements for low conductivity samples.

ACKNOWLEDGMENTS

We thank Frank Dalton, Binayak Mohanty, and David Robinson for helpful suggestions and discussions.

REFERENCES

Bertolini, D., M. Cassettari, G. Salvetti, E. Tombari, and S. Veronesi. 1991. Time domain reflectometry to study the dielectric properties of liquids—Some problems and solutions. Rev. Sci. Instrum. 62: 450–456.

Buchner, R., G.T. Hefter, and P.M. May. 1999. Dielectric relaxation of aqueous NaCl solutions. J. Phys. Chem. 103:1–9.

Cole, R.H., S. Mashimo, and P. Winsor. 1980. Evaluation of dielectric behavior by time domain spectroscopy. 3. Precision difference methods. J. Phys. Chem. 84:786–793.

Cole, R.H., and P. Winsor. 1982. Fourier transform dielectric spectroscopy. p. 183–206. *In* Alan G. Marshall (ed.) Fourier, Hadamard and Hilbert Transform in Chemistry. Plenum Press, New York.

Dalton, F.N. 1992. Development of time-domain reflectometry for measuring soil water content and bulk soil electrical conductivity. p. 143–167. *In* G. Clarke et al. (ed.) Advances in measurements of soil physical properties: Bringing theory into practice. SSSA Spec. Publ. No. 30. SSSA, Madison, WI.

Dalton, F.N., W.N. Herkelrath, D.S. Rawlins, and J.D. Rhoades. 1984. Time domain reflectometry: Simultaneous measurements of soil water content and electrical conductivity with a single probe. Science 224:989–990.

Dalton, F.N., and M.Th. van Genuchten. 1986. The time-domain reflectometry method for measuring soil water content and salinity. Geoderma 38:237–250.

Fellner-Feldegg, H. 1969. The measurement of dielectrics in time domain. J. Phys. Chem. 73:613–623.

Feng, W., C.P. Lin, R.J. Deschamps, and V.P. Drnevich. 1999. Theoretical model of a multisection time domain reflectometry measurement system. Water Resour. Res. 35:2321–2331.

Friedman, S.P., and N.A. Seaton. 1998. Critical path analysis of the relationship between permeability and electrical conductivity of three-dimensional pore networks. Water Resour. Res. 34:1703–1710.

Giese, K., and R. Tiemann. 1975. Determination of the complex permittivity form thin-sample time domain reflectometry. Improved analysis of the step response waveform. Molecular Relaxation Processes 7:45–59.

Grant, I.S., and W.R. Phillips. 1990. Electromagnetism. Wiley Interscience, Chichester, England.

Heimovaara, T.J. 1992. Comments on "Time domain reflectometry measurements of water content and electrical conductivity of layered soil columns". Soil Sci. Soc. Am. J. 56:1657–1658.

Heimovaara, T.J. 1994. Frequency domain analysis of time domain reflectometry waveforms.1. Measurement of the complex dielectric permittivity of soils. Water Resour. Res. 30:189–199.

Heimovaara, T.J., A.G. Focke, W. Bouten, and J.M. Verstraten. 1995. Assessing temporal variations in soil water composition with time domain reflectometry. Soil Sci. Soc. Am. J. 59:689–698.

Huisman, J.A., and W. Bouten. 1999. Comparison of calibration and direct measurement of cable and probe properties in time domain reflectometry. Soil Sci. Soc. Am. J. 63:1615–1617.

Mualem, Y., and S.P. Friedman. 1991. Theoretical prediction of electrical conductivity in saturated and unsaturated soil. Water Resour. Res. 27:2771–2777.

Nadler, A., S. Dasberg, and I. Lapid. 1991. Time domain reflectometry measurements of water content and electrical conductivity of layered soil columns. Soil Sci. Soc. Am. J. 55:938–943.

Nozaki, R., and T.K. Bose. 1990. Broadband complex permittivity measurements by time-domain spectroscopy. IEEE Trans. Instrum. Meas. 39:945–951.

Purvance, D.T., and R. Andricevic. 2000. On the electrical-hydraulic conductivity correlation in aquifers. Water Resour. Res. 36:2905–2913.

Reece, C.F. 1998. Simple method for determining cable length resistance in time domain reflectometry systems. Soil Sci. Soc. Am. J. 62:314–317.

Sinnema, W. 1979. Electronic transmission technology: Lines, waves, and antennas. Prentice-Hall, Englewood Cliffs, NJ.

Spaans, E.J.A., and J.M. Baker. 1993. Simple baluns in parallel probes for time domain reflectometry. Soil Sci. Soc. Am. J. 57:668–673.

Topp, G.C., J.L. Davis, and A.P. Annan. 1980. Electromagnetic determination of soil water content: Measurement in coaxial transmission lines. Water Resour. Res. 16:574–582.

Topp, G.C., V. Zasovenko, S.J. Zegelin, and S.J. Zegelin. 1988. Determination of electrical conductivity using time domain reflectometry: Soil and water experiments in coaxial lines. Water Resour. Res. 24:945–952.

Wolff, E.A., and R. Kaul. 1988. Microwave engineering and systems applications. Wiley Interscience, New York.

Yanuka, M., G.C. Topp, S.J. Zegelin, and W.D. Zebchunk. 1988. Multiple Reflection and Attenuation of time domain reflectometry pulses: Theoretical considerations for applications to soil and water. Water Resour. Res. 24:939–944.

Yeung, P.S. 1993. Lossy transmission lines—Time domain formulation and simulation model. IEEE Trans. Microwave Theory. 41:1275–1279.

Zegelin, S.J., I. White, and D.R. Jenkins. 1989. Improved field probes for soil water content and electrical conductivity measurement using time domain reflectometry. Water Resour. Res. 25:2367–2376.